ISSN 0001-4338, Izvestiya, Atmospheric and Oceanic Physics, 2017, Vol. 53, No. 9, pp. 1081–1087. © Pleiades Publishing, Ltd., 2017.
Original Russian Text © Le Hung Trinh, V.R. Zablotskii, 2016, published in Issledovanie Zemli iz Kosmosa, 2016, No. 5, pp. 42–49.

THE USE OF SPACE INFORMATION ABOUT THE EARTH

The Application of LANDSAT Multi-Temporal Thermal Infrared Data to Identify Coal Fire in the Khanh Hoa Coal Mine, Thai Nguyen province, Vietnam[1]

Le Hung Trinh[a], * and V. R. Zablotskii[b]

[a] *Le Quy Don Technical University, Hanoi, Vietnam*

[b] *Moscow State University of Geodesy and Cartography, Moscow, Russia*

**e-mail: trinhlehung125@gmail.com*

Received July 21, 2015

Abstract—The Khanh Hoa coal mine is a surface coal mine in the Thai Nguyen province, which is one of the largest deposits of coal in the Vietnam. Numerous reasons such as improper mining techniques and policy, as well as unauthorized mining caused surface and subsurface coal fire in this area. Coal fire is a dangerous phenomenon which affects the environment seriously by releasing toxic fumes which causes forest fires, and subsidence of infrastructure surface. This article presents study on the application of LANDSAT multi-temporal thermal infrared images, which help to detect coal fire. The results obtained in this study can be used to monitor fire zones so as to give warnings and solutions to prevent coal fire.

Keywords: coal fire, remote sensing, thermal infrared, LANDSAT, land surface temperature

DOI: 10.1134/S0001433817090183

INTRODUCTION

Located in Southeast Asia, Vietnam is rich in mineral resources – precious potential resource for the country. Vietnam has big reserves of fossil energy with 10 billion tons of anthracite coal, more than 200 billion tons of brown coal in the northern delta area (Luu Duc Hai and Nguyen Thi Hoang Lien, 2009). As most coal producing countries, Vietnam also has a serious coal fire problem, like USA, South Africa, Venezuela, China and India. Recently, a number of coal fires have occurred in Vietnam in the Nong Son coal mine (Quang Nam province, in 2014), Quang Ninh (in 2011) and Khanh Hoa coal mine (Thai Nguyen province, in 2014).

Remote sensing technique has many advantages in comparison to the more traditional methods for fire detection and can be effectively used for coal fire monitoring (Bondur, 2011, 2015; Bondur and Ginzburg, 2016; Bondur, 2010).

A pioneer work in this direction was executed in the USA in 1963. Since then, thermal infrared image has proven to be a reliable and useful tool for identifying subsurface coal fires. In the studies (Cracknell and Mansor, 1992; Prakash and Gupta, 1999), the authors used Landsat 5 TM thermal infrared band to identify surface and subsurface fires in Jharia coalfields (India) and calculate the area of surface fires. In the study (Voigt et al., 2004), the authors described and integrated satellite image approach for detection and monitoring of near surface coal seam fires by observing subtle land surface changes induced by the fires. The authors of study (Prasun et al., 2005) used Landsat 5 TM thermal band data for calculating surface temperature along with NDVI to identify coal fire in the Raniganj coalbelt, India. Chen et al. used multi-temporal thermal infrared data, high spatial resolution remote sensing data and field measurements to detect coal fires dynamics in the Inner Mongolia Autonomous region in northern China (Chen et al., 2007). Gautam et al. used NOAA/AVHRR data to detect the surface hot spot of Jharia coalfield region by developing an algorithm to find out the subsurface hot spot with operational satellite data (Gautam et al., 2008). Mishra et al. estimated of air pollution concentration over Jharia coalfield and established a relation between satellite imagery and ground data (Mishra et al., 2013). Based on this study, Mishra proved that, the eastern part of Jharia coalfield was more polluted in comparison to the western part due to extensive mining actives as well as a large number of coal fires. Mishra et al. found a correlation between satellite image temperature and surface temperature of the Jharia coalfield (Mishra et al., 2014). Hongyuan Huo et al. have identified thermal anomalies related to subsurface coal fires in the Rujigou coal basin in northwestern China (Hongyuan Huo et al., 2014).

[1] The article was translated by the authors.

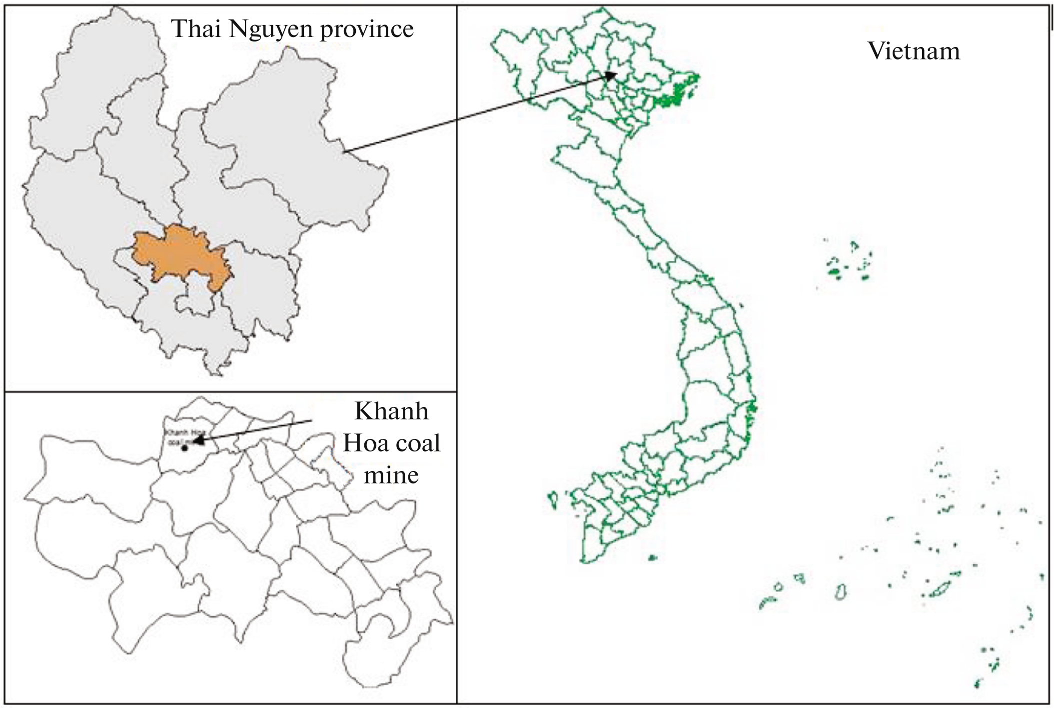

Fig. 1. The study area, Khanh Hoa coal mine, Thai Nguyen province (Vietnam).

This paper is devoted to the problem of identifying and assessing the dynamics of coal fire in Khanh Hoa coal mine, Thai Nguyen province (Vietnam) using Landsat multi-temporal thermal infrared data.

STUDY AREA

The Khanh Hoa coal mine is located in the northern of Thai Nguyen city, about 80 km northeast of Hà Noi, the capital of Vietnam (Fig. 1). The area is bounded by 21°36′7″ N latitude and 105°46′59″E longitude. Thai Nguyen is located on the territory with smooth relief, typical for the central counties. In the western part of the city there are small areas occupied by woody vegetation. The main species of vegetation are afforestation, consisting mainly of tea trees.

Coal mining is an important contributor to the development of local social economy, but also has negative impact on the environment, such as water and air pollution, coal fire. In the recent years, there have been several coal fires in the Khanh Hoa coal mine.

DATA USED

In this study, multi-temporal cloud – free Landsat 5 TM, Landsat 7 ETM+ and Landsat 8 OLI data were collected (Figs. 2a, 2b, 2c). All the Landsat data were the standard terrain correction products (L1T), downloaded from United States Geological Survey (USGS – http://glovis.usgs.gov) website. These images were taken in the dry season when cloudless skies. The data used in this study was grouped into two categories (Table 1), the thermal infrared data was used to calculate surface emissivity based on normalized difference vegetation index (NDVI).

METHODOLOGY

Conversion of the Digital Number to Spectral Radiance

Image processing started with radiometric and geometric correction. In first step, the brightness of the pixel value (digital number) is converted into the spectral radiance value (Wm^{-2} μm^{-1}). The spectral radiance values of Landsat 5 TM and Landsat 7 ETM+ images were calculated using a model devel-

Table 1. The Landsat multispectral images used in this study

No.	Data type	Band used for temperature	Band used for NDVI	Time of data acquisition
1	Landsat 7 ETM+	6	3, 4	November 8, 2007
2	Landsat 5 TM	6	3, 4	November 8, 2010
3	Landsat 8 OLI	10	4, 5	January 19, 2014

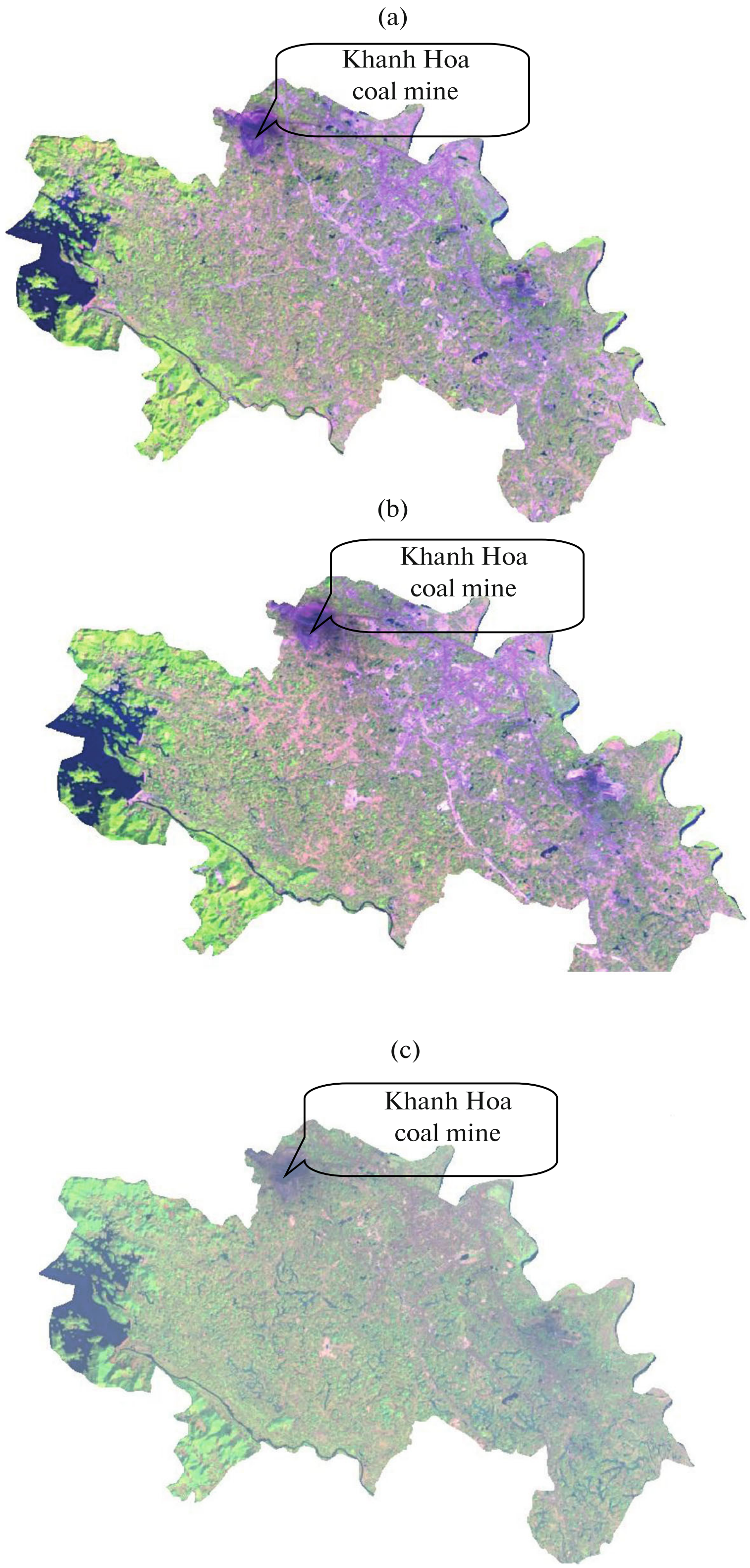

Fig. 2. Landsat multispectral images of the Thai Nguyen city received on (a) November 8, 2007, (b) November 8, 2010, and (c) January 19,2014.

Table 2. Landsat TM and ETM+ spectral radiance $L\max_\lambda$, $L\min_\lambda$ dynamic ranges [14]

No.	Data type	Band	$L\max_\lambda$	$L\min_\lambda$
1	Landsat 7 ETM+	6.1 Low gain	17.04	0.0
		6.2 High gain	12.65	3.2
2	Landsat 5	6	15.3032	1.2378

Table 3. Landsat 8 TIRS spectral radiance M_L, A_L dynamic ranges [14]

No.	Data type	Band	M_L	A_L
1	Landsat 8 TIRS	10	3.3420×10^{-4}	0.10000
2	Landsat 8 TIRS	11	3.3420×10^{-4}	0.10000

oped by NASA (Landsat-7 Science Data User's Handbook):

$$L_\lambda = \frac{L\max_\lambda - L\min_\lambda}{Q_{\text{cal max}} - Q_{\text{cal min}}}(Q_{\text{cal}} - Q_{\text{cal min}}) + L\min_\lambda, \quad (1)$$

where L_λ—spectral radiance at the sensor's aperture [W/(m^2 sr μm)]; Q_{cal}—quantized calibrated pixel value; $Q_{\text{cal max}}$—Maximum quantized calibrated pixel value corresponding to $L\max_\lambda$; $Q_{\text{cal min}}$—minimum quantized calibrated pixel value corresponding to $L\min_\lambda$; $L\max_\lambda$—spectral at sensor radiance that is scaled to DNmax [W/(m^2 sr μm)]; $L\min_\lambda$—spectral at-sensor radiance that is scaled to DNmin [W/(m^2 sr μm)].

For the Landsat 8 OLI data, L_λ is determined by the following formula:

$$L_\lambda = M_L Q_{\text{cal}} + A_L, \quad (2)$$

where M_L, A_L—band specific multiplicative rescaling factor from the metadata (RADIANCE_MIUL_BAND_x and RADIANCE_ADD_BAND_x); Q_{cal}—quantized and calibrated standard product pixel values (interger).

Conversion of the Spectral Radiance to Brightness Temperature

At the second step, the surface brightness temperature was determined. The surface brightness temperature of Landsat thermal infrared data was calculated using following formula:

$$T = \frac{K_2}{\ln\left(\frac{K_1}{L_\lambda} + 1\right)}, \quad (3)$$

where T—at satellite brightness temperature (K); K_1—calibration constant 1 [W/(m^2 sr μm)]; K_2—calibration constant 2 [K].

Estimation of Surface Emissivity

To determine the land surface temperature, it is necessary to know the surface emissivity coefficient ε. In this paper, the surface emissivity is determined by using method, which proposed by Valor and Caselles (Valor, Caselles, 1996) by following equation:

$$\varepsilon = \varepsilon_v P_v + \varepsilon_s(1 - P_v), \quad (4)$$

where ε—surface emissivity; ε_v—emissivity of pure vegetation covers area; ε_s—emissivity of pure soil area; P_v—the percentage of vegetation in one pixel, which calculated (Carlson and Ripley, 1997; Zhangyan Jiang et al., 2006) by equation:

$$P_v = \left(\frac{\text{NDVI} - \text{NDVI}_{\min}}{\text{NDVI}_{\max} - \text{NDVI}_{\min}}\right)^2, \quad (5)$$

where NDVI—normalized difference vegetation index:

$$\text{NDVI} = \frac{\text{NIR} - \text{RED}}{\text{NIR} + \text{RED}}, \quad (6)$$

where RED and NIR—the spectral reflectance in red and near—infrared band, respectively. $\text{NDVI}_{\max}$, $\text{NDVI}_{\min}$—the NDVI values of vegetation and open soil, which are determined experimentally using a series of test area for vegetation and open soil.

Calculation of Land Surface Temperature

In the final step, land surface temperature (LST) is estimated by the following equation:

$$LST = \frac{T}{1 + \frac{\lambda T_B}{\rho}\ln\varepsilon}, \quad (7)$$

where λ—the wavelength of the emitted radiance; constant $\rho = \frac{hc}{k}$, k—Boltzmann's constant (1.38×10^{-23} J/K), h—Plank's constant (6.626×10^{-34}J s); c—velocity of light (2.998×10^8 m/s).

RESULTS AND DISCUSSIONS

For determining surface emissivity by method of Valor and Caselles (Valor and Caselles, 1996), emissivity values of soil and vegetation are needed. This study has been used more than 100 training samples for bare soil and vegetation cover areas to calculate normalized difference vegetation index (NDVI). The minimum and maximum NDVI values of the open soil are equal to 0.122 and 0.127, and for vegetation, these values are equal 0.505 and 0.519, respectively. Finally, NDVI for pure soil and pure vegetation cover of study area equal 0.125 and 0.510, respectively. Emissivity of pure soil and pure vegetation cover areas are calculated using method of Van de Griend and Owen (Van de Griend and Owen, 1993) by following equation:

$$\varepsilon = 1.0094 + 0.047\ln(\text{NDVI}). \quad (8)$$

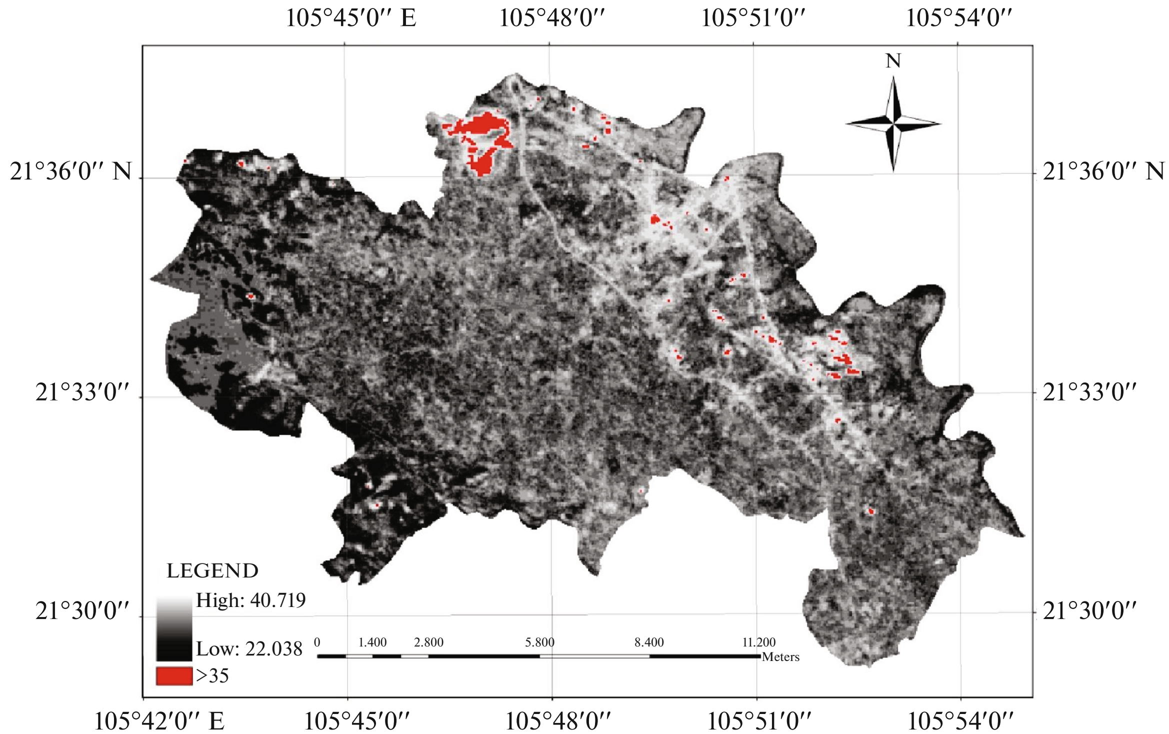

Fig. 3. Subsurface coal fire in Khanh Hoa coal mine in November 8, 2007.

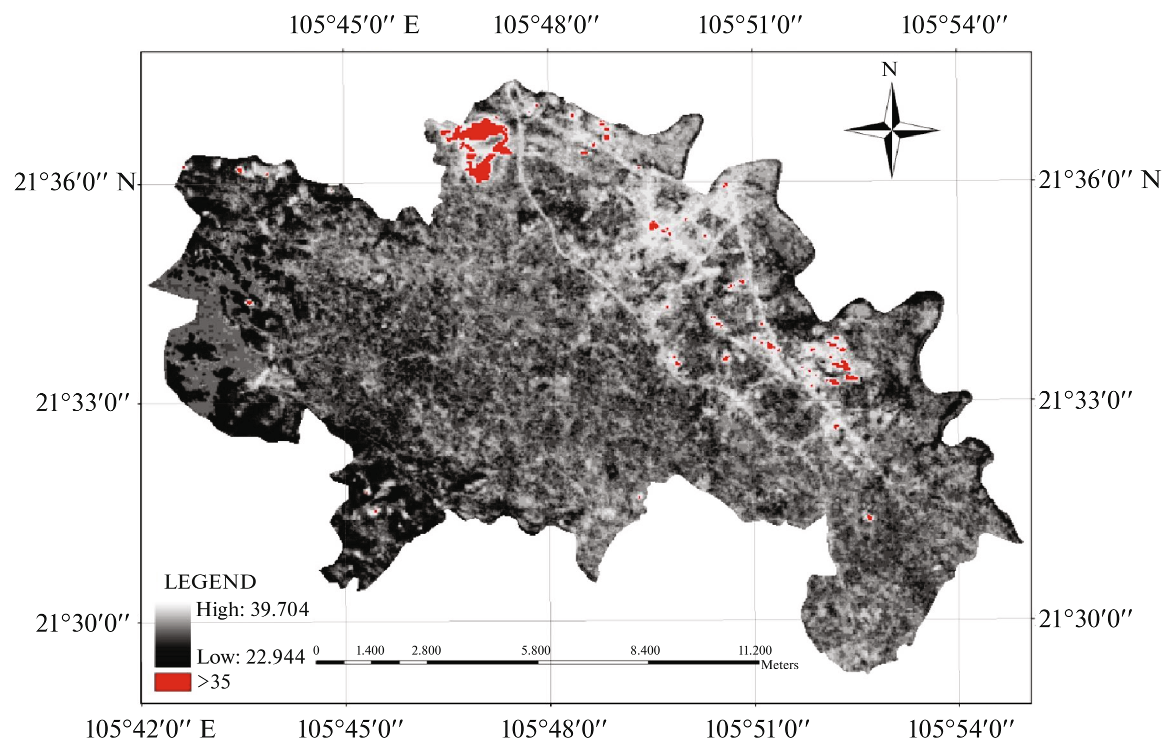

Fig. 4. Subsurface coal fire in Khanh Hoa coal mine in November 8, 2010.

Emissivity of pure soil and pure vegetation cover areas identified by using this method equal 0.912 and 0.978, respectively. The resulting materials are presented in the form of halftone map of land surface temperature distribution in the study area. In Figs. 3–5, nine zones are identified with the following tempera-

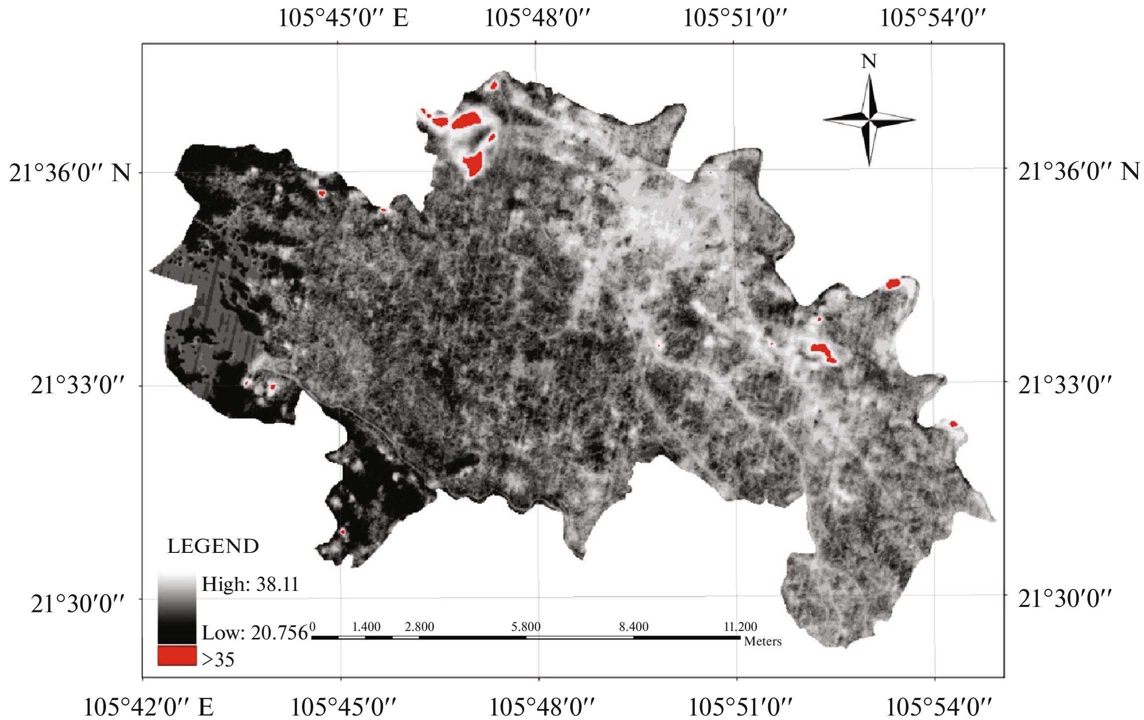

Fig. 5. Subsurface coal mine in Khanh Hoa coal mine in January 19, 2014.

tures: less than 21, 21–23, 23–25, 25–27, 27–29, 29–31, 31–33, 33–35 and greater 35°C. Areas with the surface temperature above 35°C were considered subsurface coal fire territory according to the classification of Mishra et al. (Mishra et al., 2014). Subsurface coal fires in Khanh Hoa coal mine were clearly detected in the northern part of territory. On the basis of land surface temperature image, there was a good contrast between suspected coal fire area and surroundings. Surface temperature in Khanh Hoa coal mine so much higher than in surroundings, even compare in urban area, which is characterized by impervious surfaces. Areas of prominent temperature anomalies colored in red (Figs. 3–5).

Table 4. Landsat TM, ETM+ and Landsat 8 thermal band calibration constants [14]

No.	Data type	Band	W/(m^2 sr μm)	K_2 (Kelvin)
1	Landsat 5 TM	6	607.76	1260.56
2	Landsat 7 ETM+	6	666.09	1282.71
3	Landsat 8	10	774.89	1321.08
		11	480.89	1201.14

Table 5. Subsurface coal fire area in different year calculated by Landsat data

No.	Time of data acquisition	Area of surface coal fires, ha
1	November 8, 2007	139.56
2	November 8, 2010	158.76
3	January 19, 2014	74.43

The study shows that the total coal fire affected area in Khanh Hoa coal mine was increased from 2007 to 2010 and reduced to 2014. For example, in 2007 the coal fire area was 139.56 hectares, in 2010 it increased to 158.76 hectares, and in 2014 decreased by 74.43 hectares). Thus, the total fire area increased by 13.76% for period 2007–2010 and decreased by 53.12% over the period 2010–2014.

CONCLUSIONS

Coal fire is a dangerous phenomenon which affects seriously on the environment. Land surface temperature is higher in the zones of subsurface coal fire than in their surroundings areas. Remote sensing technique can be used effectively for coal fire detecting and monitoring. In this study, multi-temporal Landsat TM, ETM+ and Landsat 8 thermal band data from 2007 to 2014 were used to calculate spectral radiance and converted to the brightness temperature. To retrieve the land surface temperature, the surface emissivity was estimated using NDVI index based on method developed by Valor, Caselles (Valor and Caselles, 1996) and Van de Grined, Owen (Van de Griend and Owen, 1993).

The dynamics of coal fires in Khanh Hoa coal mine during period of 2007–2014 were analyzed, as the result of which the coal fire areas increased from 139.56 ha in 2007 to 158.76 ha in 2010, and decreased to 74.43 ha in 2014.

The results of this study confirm the possibility of controlling coal fires using remote sensing technique for taking preventive measures, localization and prevention of coal fires. The results which are obtained in this study can be used effectively for early detection of coal fires in Khanh Hoa coal mine and their monitoring, as well as create a map of the dynamics of coal fire over the observation period.

REFERENCES

Bondur, V.G., Importance of aerospace remote sensing approach to the monitoring of nature fire in Russia, *Int. Forest Fire News*, 2010, no. 40, pp. 43–57.

Bondur, V.G., Satellite monitoring of wildfires during the anomalous heat wave of 2010 in Russia, *Izv., Atmos. Ocean. Phys.*, 2011, vol. 47, no. 9, pp. 1039–1048.

Bondur, V.G., Satellite Monitoring of Trace Gas and Aerosol Emissions during Wildfires in Russia, *Izv., Atmos. Ocean. Phys.*, 2016, vol. 52, no. 9, pp. 1078–1091.

Bondur, V.G. and Ginzburg, A.S., Emission of carbon-bearing gases and aerosols from natural fires on the territory of Russia based on space monitoring, *Dokl. Earth Sci.*, 2016, vol. 466, no. 2, pp. 148–152.

Carlson, T.N. and Ripley, D.A., On the relation between NDVI, fractional vegetation cover and leaf area index, *Remote Sens. Environ.*, 1997, vol. 62, pp. 241–252.

Chen, Y., Li, J., Yang, B., and Zhang, S., Detection of coal fire location and change based on multi-temporal thermal remotely sensed data and field measurements, *Int. J. Remote Sens.*, 2007, vol. 28, no. 15, pp. 3173–3179.

Cracknell, A.P. and Mansor, S.B., Detection of sub-surface coal fires using Landsat thematic mapper data, *Int. Arch. Photogram. Remote Sens.*, 1992, vol. 29, pp. 750–753.

Gautam, R.S., Singh, V.K., and Mittal, D., An efficient contextual algorithm to detect subsurface fires with NOAA/AVHRR data, *IEEE Trans. Geosci. Remote Sens.*, 2008, vol. 46, no. 7, pp. 2005–2015.

Huo H., Jiang X., Song, X., Li, Zh.-L., Ni, Zh., and Gao, C., Detection of coal fire dynamics and propagation direction from multi-temporal nighttime Landsat SWIR and TIR data: A case study on the Rujigou coalfield Northwest China, *Remote Sens.*, 2014, vol. 6, no. 2, pp. 1234–1259. doi 10.3390/rs6021234

Jiang, Z., Huete, A.R., Chen, J., Chen, Y., Li, J., Yan, G., et al., Analysis of NDVI and scaled difference vegetation index retrievals of vegetation fraction, *Remote Sens. Environ.*, 2006, vol. 101, no. 3, pp. 366–378. doi 10.1016/j.rse.2006.01.003

Landsat-7 Science Data User's Handbook, Greenbelt, MD: NASA/Goddard Space Flight Center.

Luu, D.H. and Nguyen, T.H.L., Renewable energy policies for sustainable development in Vietnam, *VNU J. Sci.: Earth Sci.*, 2009, vol. 25, no. 3, pp. 133–142.

Mishra, R.K., Pandey, J., Chaudhary, S.K., Khalkho, A., and Singh, V.K., Estimation of air pollution concentration over Jharia coalfield based on satellite imagery of atmospheric aerosol, *Int. J. Geomatics Geosci.*, 2013, vol. 4, no. 1, pp. 30–35.

Mishra, R.K., Roy, P.N.S., Pandey, J., Khalkho, A., and Singh, V.K., Study of coal fire dynamics of Jharia coalfield using satellite data, *Int. J. Geomatics Geosci.*, 2014, vol. 4, no. 3, pp. 477–484.

Prakash, A. and Gupta, R.P., Surface fires in Jharia coalfield, India—their distribution and estimation of area and temperature from TM data, *Int. J. Remote Sens.*, 1999, vol. 20, pp. 1935–1946.

Prasun, K., Kuntala, L., and Kanika, S., Application of remote sensing to identify coalfires in the Raniganj Coalbelt, India, *Int. J. Appl. Earth Obs. Geoinform.*, 2006, vol. 8, no. 3, pp. 188–195. doi 10.1016/j.jag.2005.09.001

Valor, E. and Caselles, V., Mapping land surface emissivity from NDVI. Application to European, African and South American areas, *Remote Sens. Environ.*, 1996, vol. 57, pp. 167–184.

Van de Griend, A.A. and Owen, M., On the relationship between thermal emissivity and the normalized difference vegetation index for natural surface, *Int. J. Remote Sens.*, 1993, vol. 14, pp. 1119–1131.

Voigt, S., Tetzlaff, A., Zhang, J., Kunzer, C., Zhukov, B., and Strunz, G., Integrating satellite remote sensing techniques for detection and analysis of uncontrolled coal seam fire in North China, *Int. J. Coal Geol.*, 2004, vol. 59, nos. 1–2, pp. 121–136. doi 10.1016/j.coal.2003.12.013